Journal of Alloys and Compounds 508 (2010) 412–418

Contents lists available at ScienceDirect

Journal of Alloys and Compounds

journal homepage: www.elsevier.com/locate/jallcom

Influence of the current flow on the SPS sintering of a Ni powder

L. Minier[a], S. Le Gallet[a,*], Yu. Grin[b], F. Bernard[a]

[a] Laboratoire Interdisciplinaire Carnot de Bourgogne, UMR 5209 CNRS-UB, 9 Av. Alain Savary, BP 47870, 21078 Dijon Cedex, France
[b] Max-Planck-Institut für Chemische Physik fester Stoffe, NÖthnitzer Straße 40, 01187 Dresden, Germany

ARTICLE INFO

Article history:
Received 25 February 2010
Received in revised form 5 August 2010
Accepted 17 August 2010
Available online 27 August 2010

Key words:
Metals and alloys
Sintering
Microstructure
Metallography

ABSTRACT

A nickel powder with the particle size 4.3 μm has been sintered, using a SPS apparatus, by identical set temperature, heating rate, dwell time and pressure in different moulds: (a) with graphite die and punches, (b) with alumina die and graphite punches and (c) with graphite die and punches including alumina spacers between punches and powder. Although all set sintering parameters are identical, the microstructure of the resulted nickel specimens depends on the moulds. The bulk density is higher when an alumina die is used. On the contrary, the bulk microstructure does not seem to be influenced by the graphite foil presence, generally used between the system parts. The present paper is an attempt to correlate the bulk microstructure evolution with the electric and thermal characteristics of the moulds and graphite foil, and the resulted current flow.

1. Introduction

Spark Plasma Sintering (SPS) is a powder metallurgy processing for consolidation of a large variety of materials in a short time [1–3]. Contrary to conventional sintering, the grain growth is limited [4–6]. In the SPS process, a uniaxial pressure combined with a pulsed electric current is applied. Thus, the current flow should be strongly dependent on the characteristics of the different elements which compose the system (powder, punches, die) and, particularly, their electrical and thermal characteristics. The Joule effect of the powder can lead locally to very high temperatures. For example, the shape of necks formed during the sintering of a copper powder at 600 °C indicates that the temperature was in fact locally (in the necks) close to its melting point (1084 °C) [7]. That is why a very detailed attention has to be taken to the temperature value because the temperature which checks the electric power is measured inside the die (at the external surface or inside a hole). Consequently, the temperature of the sample is not really determined. This is all the more true as there is a temperature gradient between the die and the sample. Owing to the electric characteristics of the powder and the sintering temperature, the die temperature is superior or inferior to that of the sample. Matsugi et al. [8] have shown that the temperature of a titanium powder is superior to that measured in the die. On the contrary, in the case of an alumina powder, its temperature is inferior to the die temperature. In addition, Kamiya [9] has shown that in the case of a carbon powder electrically insulated by a liner of boron nitride from the punches, the die temperature is 100 °C higher than that of the sample for low sintering temperatures (870 °C) but is 100 °C lower for higher ones (1500 °C). Schmidt [10] has also observed an effect of the thermal insulation on the thermal gradient. For a sintering at 900 °C, the temperature difference between the sample and the die is 90 °C for an alumina powder and 105 °C for a molybdenum powder. This gradient is only 15 °C and 40 °C respectively with a thermal insulation around the die. More generally, the temperature gradient also depends on the heating rate, the pressure, the geometry and the electric characteristics of the die, the chamber volume, the atmosphere... [11,12].

From a practical point of view, a graphite foil is inserted between all parts of the system. Indeed, it ensures good physical, electric and thermal contacts [13]. However, modelling of contact resistance is very difficult. Anselmi-Tamburini et al. [14] have modelled the current and temperature distributions in an idealised system, where no contact resistance is taken into account and, all the graphite components (die and punches) are considered as a continuous piece. Vanmeensel et al. [15] have studied the thermal and electrical contact resistances introduced by horizontal and vertical graphite foils. They have shown that the temperature difference between a central and an external pyrometer for different graphite dummies is strongly dependent on the presence of the vertical graphite foil. They have also observed that the temperature recorded by the external pyrometer starts to differ significantly from the temperature recorded by the central one in the case of the sintering of a powder compact when this latter starts to be dense [15]. Zavaliangos et al. [16] have reported that an electrical and thermal contact resistance has to be introduced for a proper description of the inter-

* Corresponding author. Tel.: +33 380396163; fax: +33 380396167.
E-mail address: sophie.le-gallet@u-bourgogne.fr (S. Le Gallet).

0925-8388/$ – see front matter © 2010 Elsevier B.V. All rights reserved.
doi:10.1016/j.jallcom.2010.08.077

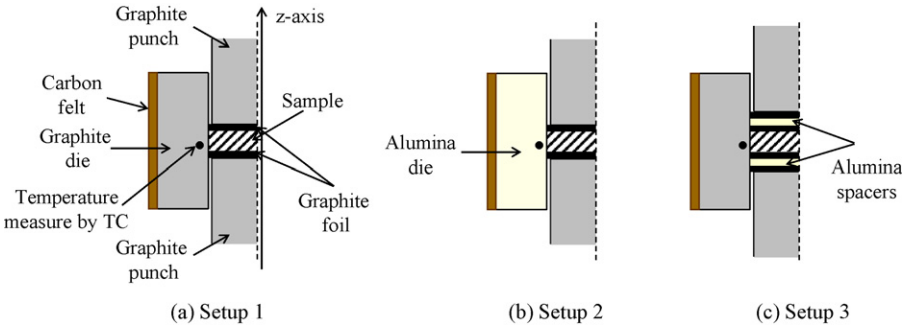

Fig. 1. Mould setups to study the influence of die and punch electric characteristics on the microstructure of sintered nickel: (a) graphite die and punches (setup 1), (b) alumina die and graphite punches (setup 2) and (c) graphite die and punches with alumina spacers between sample and punches (setup 3).

faces in the finite element models in order to match simulated results with experimental data.

In this study, the influence of the electric characteristics of the mould and of the graphite foil on the system resistance has been experimentally investigated for the sintering of a conducting powder such as nickel.

2. Experimental procedure

The investigation has been performed by comparing the electric power delivered by the SPS apparatus and the bulk microstructure for different mould and graphite foil setups. In all experiments, the sintering temperature is fixed, only the electric power may change to heat the system at this temperature. The electric power is determined by the product of the voltage $U(t)$ and the current $I(t)$ recorded during the thermal cycle.

A nickel powder (Alfa aesar, 99.9%) with a mean particle size of $4.3 \pm 1.5\,\mu m$ has been selected. For each experiment, about 3.1 g of powder were poured into a cylindrical die (15 mm inner diameter, 30 mm outer diameter and 30 mm height) surrounded by a carbon felt (to reduce the radiation heat losses from the outer wall). The powder was consolidated using a SPS-515S apparatus (Syntex Inc.) with a pulse sequence of 12:2 ms (on:off). The temperature was monitored by a K-type thermocouple set in the die wall at 2 mm far from the sample and half height of the die.

Firstly, the sintering experiments were carried out with graphite foils, inserted between the powder and the punches. Three setups have been investigated (Fig. 1). In the first one (setup 1), the nickel powder is sintered in a graphite die. In the second one (setup 2), the sintering is performed in an alumina die in order to evaluate the influence of the electric and thermal die characteristics on the powder heating, which is mainly ensured by Joule effect. Finally, to evaluate the heating of the powder only by thermal conduction, the powder is electrically and thermally insulated from the punches by alumina spacers in a setup 3. All samples were sintered at 750 °C under a pressure of 15 MPa with a heating rise of 50 °C/min during 10 min. Other sintering conditions in terms of heating rate or pressure have not been investigated due to the low thermal conductivity and the insufficient mechanical properties of the alumina die.

To investigate the influence of the graphite foil, the sintering experiments were performed in a graphite mould with a graphite foil of 0.2 mm thickness inserted or not between the different parts of the system. The various setups are presented in Fig. 2. Contrary to the setup 4 where graphite foils are introduced between all parts of the system, the setup 6 does not contain graphite foil. In the setup 6, it has been considered that there is no physical contact between punch and die because the tilt of the die during the pressing is unlikely. Indeed, the punches (20 mm in length) are inserted of 10 mm in the die before the sintering and of 15 mm after the sintering. Finally, the sintering in the setup 5 was realised with graphite foils only between the powder and the punches (it is exactly the same setup as setup 1, renamed for more clarity). The samples were sintered at 750 °C during 10 min. The graphite foil effect has been evaluated by varying the heating rate (50 and 200 °C/min) and the pressure (30 and 70 MPa). Indeed, as the pressure can modify the electrical resistance of conducting samples, the current (and consequently the temperature) distribution depends on the mechanical pressure applied [17,18].

Table 1 gives the electrical resistivity and the thermal conductivity of the different system parts.

Bulk densities (noted d in the figures) of the sintered samples were determined using Archimedes method in water. Each value is an average of four measurements. Sample microstructures were observed, after polishing and chemical etching with an acid solution of copper sulfate, using an optical microscope (Axiovert 100A). The grain size (noted G in the figures) is determined by accounting for 300 grains on several pictures around the sample centre (using the intercept method).

3. Results

3.1. Influence of the mould setup

Fig. 3 shows the electric power delivered according to the die and punch electric characteristics. During the heating rise, the electric power in the setups 1 and 2 are similar and higher than that in the setup 3. During the dwell time, the electric power delivered in an alumina die (setup 2) is higher than the electric power delivered in a graphite die with alumina spacers between the powder and the punches (setup 3) but, lower than the electric power delivered in a graphite die (setup 1). As expected, the electric power provided by the SPS apparatus is function of the die and punch electric characteristics despite a set sintering temperature in the three cases.

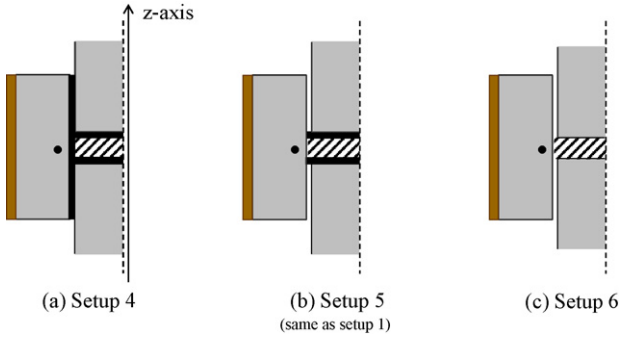

Fig. 2. Graphite foil setups to study the influence of the graphite foil presence on the microstructure of sintered nickel: (a) classical (setup 4), (b) with graphite foil only between sample and punches (setup 5) and (c) without graphite foil (setup 6).

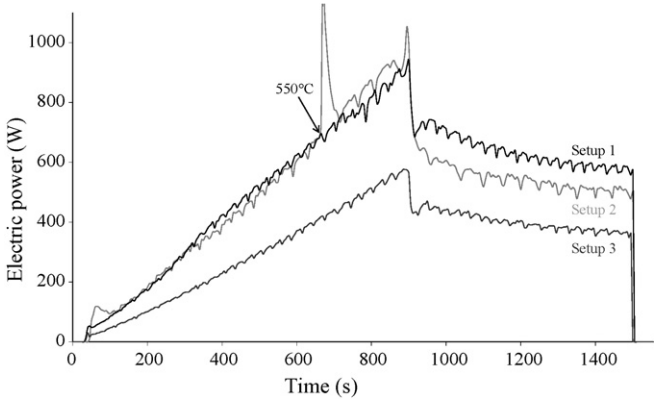

Fig. 3. Electric power delivered as a function of the mould setup for a sintering cycle of 750 °C under a pressure of 15 MPa with a heating rate of 50 °C/min during 10 min.

Table 1
Electric and thermal characteristics of the mould and the graphite foil.

	Graphite die/punches[a]	Alumina die/spacers[b]	Graphite foil[a]	
			Along [1 0 0]	Along [0 0 1]
Electric resistivity (Ω cm)	1.6×10^{-3}	10^{14}	0.001	0.05
Thermal conductivity (W/m/K)	80	26–35	160	4

[a] Carbone Lorraine data.
[b] BCE Special Ceramics GmbH data.

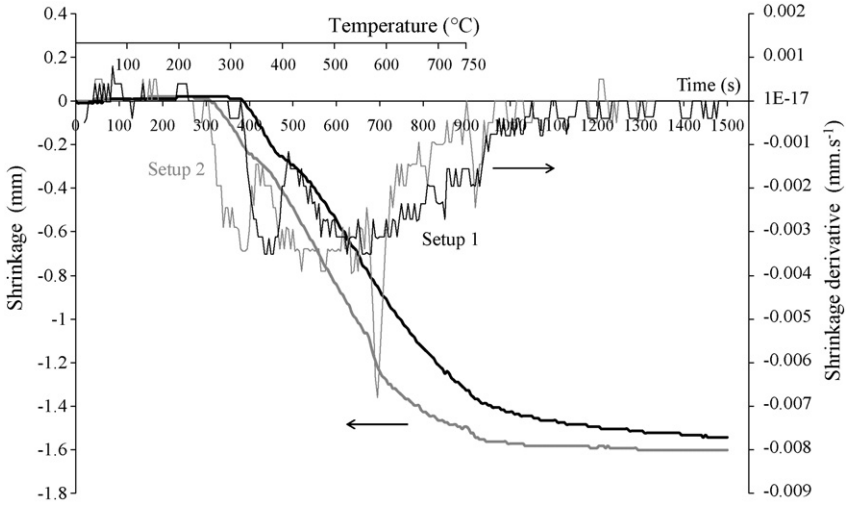

Fig. 4. Shrinkage and shrinkage rate curves of a nickel sample sintered at 750 °C under a pressure of 15 MPa with a heating rate of 50 °C/min during 10 min in a graphite die (setup 1) and in an alumina die (setup 2).

Moreover, an electric power peak is observed at about 550 °C in the case of the sintering of the nickel powder in an alumina die (setup 2). This peak coincides with the radial breaking of the die into two parts. The density of a sample sintered at 540 °C in an alumina die with a heating rate of 50 °C/min under a pressure of 15 MPa without dwell time is only 71.3%. Consequently, the die breaking cannot be explained by the sample dilatation but may simply have for origin the poor thermal shock resistance of alumina.

Fig. 4 shows the shrinkage and shrinkage rate curves versus time of the nickel sintered in the setups 1 and 2. The curves are shifted towards the high temperatures when, for the die, graphite is used instead of alumina.

Fig. 5 shows the variation of the sample relative densities and the microstructure evolution according to the die and punch characteristics. The highest density (94.5%) and grain size (12 μm) are obtained for a sintering in the alumina die

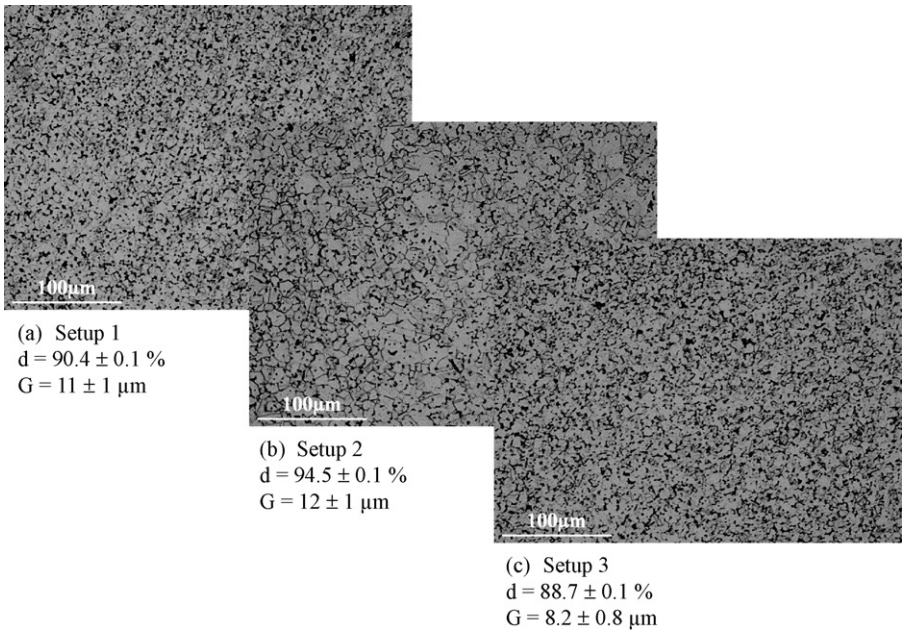

Fig. 5. Microstructure of nickel specimens sintered at 750 °C under a pressure of 15 MPa with a heating rate of 50 °C/min during 10 min in (a) a graphite die (setup 1), (b) an alumina die (setup 2) and (c) a graphite die with alumina spacers between sample and punches (setup 3).

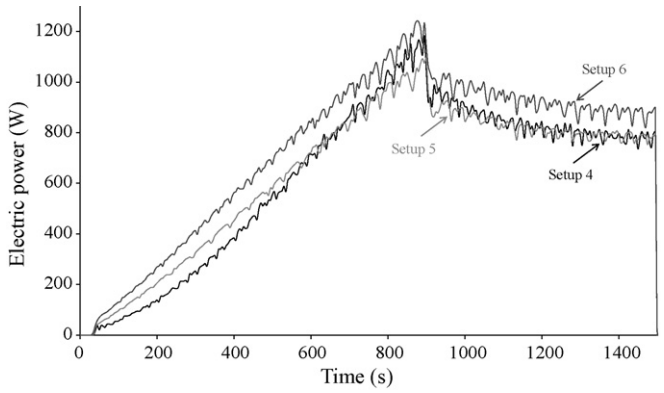

Fig. 6. Electric power delivered as a function of graphite foil setup for a sintering cycle of 750 °C under a pressure of 70 MPa with a heating rate of 50 °C/min during 10 min.

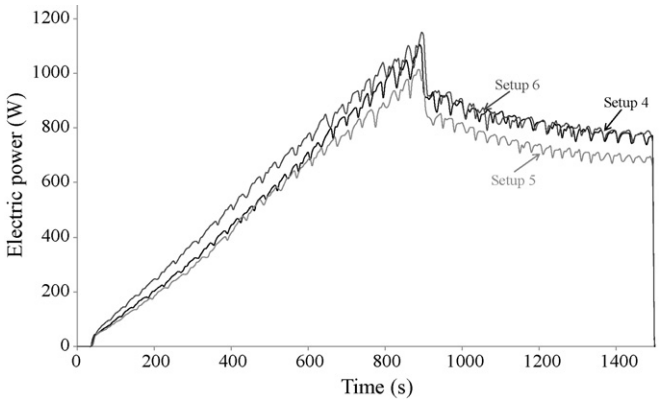

Fig. 7. Electric power delivered as a function of graphite foil setup for a sintering cycle of 750 °C under a pressure of 30 MPa with a heating rate of 50 °C/min during 10 min.

whereas the lowest ones (88.7% and 8.2 μm respectively) are obtained for a sintering in the graphite die with alumina spacers.

3.2. Influence of the graphite foil setup

The electric power curves according to the graphite foil setups are presented in Fig. 6 for samples sintered with a 50 °C/min heating rate under 70 MPa. The electric powers delivered for setups 4 and 5 are considered equivalent and lower than that for the setup 6. However, when the pressure is lowered to 30 MPa, the electric power delivered for the setup 4 becomes equivalent to that delivered for the setup 6. Setup 5 delivers the lowest electric power (Fig. 7).

Fig. 8 shows the sample microstructure according to the graphite foil setup. No density dependence was found on the graphite foil setup, contrary to the previous results on the mould setup. The obtaining of dense compacts under 70 MPa (97.6–97.9%) makes probably more difficult the observation of the setup effect on the final density. But, under a pressure of 30 MPa (200 °C/min), no influence has been also observed even if with relative densities lower than 94%, the samples are not totally densified (Table 2). The sintering without the graphite foil (setup 6) seems to lead to specimens with slightly larger grains whatever the pressure and the heating rate.

4. Discussion

4.1. Preliminary

The present discussion is mainly based on Joule effect and thermal conductivity considerations because the primary role of the electric field is thermal through Joule heating. Although the SPS controller adjusts the used voltage as a variable function of the overall resistivity of the setup and controls the current for heating, the voltage does almost not vary from one setup to another (Fig. 9). As the applied voltage is quite similar in all setups, the influence of the field on mass transport has not been taken into account to explain the microstructure variations of the nickel specimens. On the contrary, Joule heating and the heat exchanges between the different parts of the system change. That is why the sample temperature might be different from one setup to another.

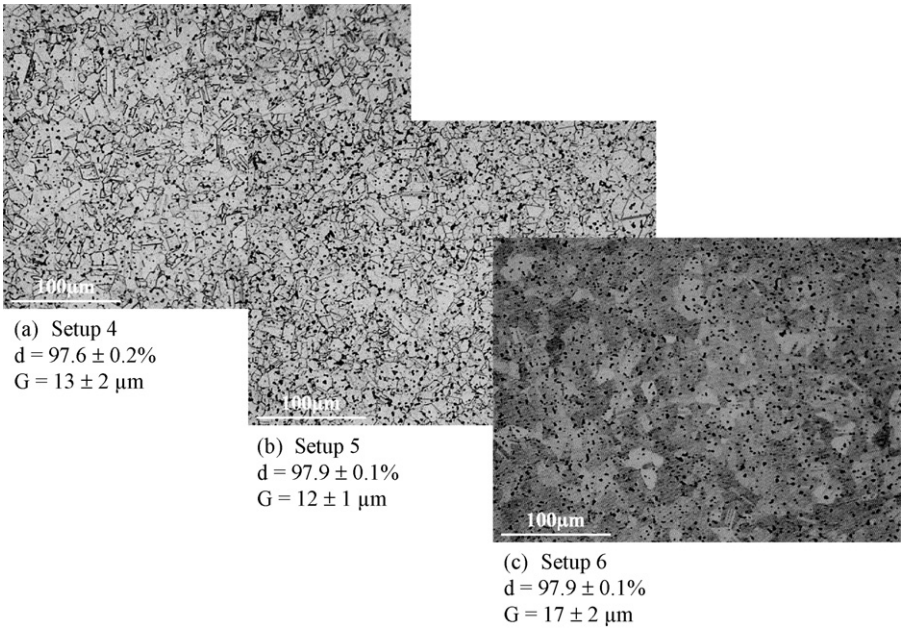

Fig. 8. Microstructure of nickel specimens sintered at 750 °C under a pressure of 70 MPa with a heating rate of 50 °C/min during 10 min (a) with graphite foil between sample and punches and between sample and die (setup 4), (b) with graphite foil only between sample and punches (setup 5) and (c) without graphite foil (setup 6).

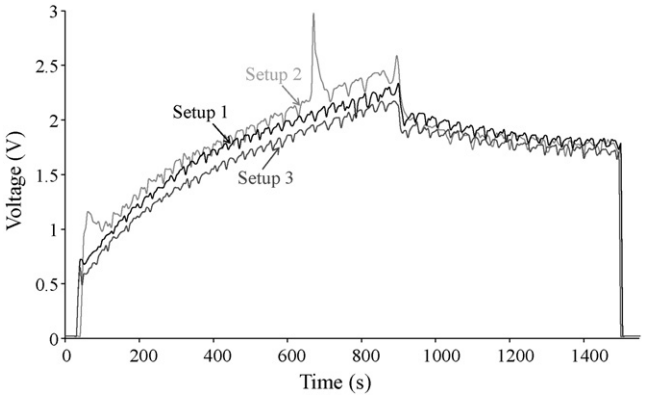

Fig. 9. Voltage delivered as a function of the mould setup for a sintering cycle of 750 °C under a pressure of 15 MPa with a heating rate of 50 °C/min during 10 min.

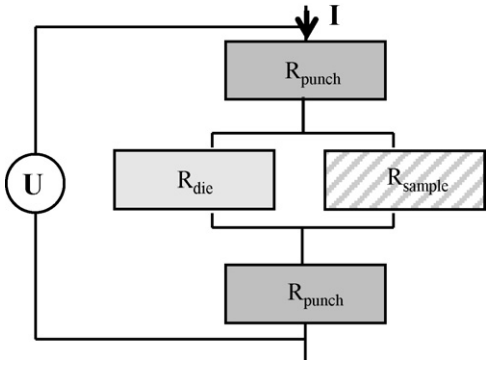

Fig. 10. Equivalent electric scheme of the SPS setup.

The system composed of punches, die and sample can be assimilated to an association of resistances which can be in parallel or in series according to the die and sample electric characteristics (Fig. 10). The equivalent scheme (Fig. 10) does not take into account the graphite foil inserted between the different parts of the system. Due to the good electric characteristics of the graphite foil (Table 1), its electric resistance is 100 times higher than that of nickel sample ($\rho = 6.9 \times 10^{-6}\ \Omega$ cm) but even if the graphite foil exhibits a relative large Joule heating, due to its small volume, the resulting effect on the spatial temperature variation is limited [16]. A general heat balance, taken into account the heat produced on the one hand, by Joule effect and, on the other hand, the heat transfers between each element composing the system, can be schematized as proposed in Fig. 11. The arrows, represented in Fig. 11b, symbolise the

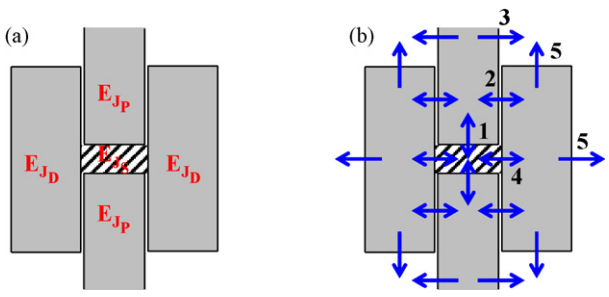

Fig. 11. (a) Joule effects (E_{JS}, E_{JP} and E_{JD} correspond to Joule effects of the sample, the punches and the die respectively) and (b) thermal energy transfers between the different system parts ($E_{th\ P\leftrightarrow S}$ (1), $E_{th\ P\leftrightarrow D}$ (2), $E_{th^*\ P\rightarrow O}$ (3), $E_{th\ D\leftrightarrow S}$ (4), $E_{th^*\ D\rightarrow O}$ (5) correspond to heat transfers by conduction between punches and sample, punches and die, by radiation from punches to outside, by conduction between die and sample and, by radiation from die to outside respectively).

Table 2
Influence of the graphite foil on the characteristics of nickel bulks under different sintering conditions.

Sintering conditions	Setup	Relative density (%)	Grain size after sintering (μm) (microscope data)
200 °C/min, 30 MPa	4	93.8 ± 0.1	11 ± 1
	5	93.8 ± 0.1	9 ± 1
	6	94.0 ± 0.1	15 ± 2
200 °C/min, 70 MPa	4	97.7 ± 0.1	10 ± 2
	5	98.1 ± 0.1	12 ± 2
	6	97.8 ± 0.1	13 ± 2

heat transfer between the different elements of the system without taking into account the quantities of thermal energy exchanged.

The thermal characteristics of the graphite foil are different from those of the die and punches (Table 1). Its presence may consequently modify the heat exchanges between the die and the sample on the one hand, and between the punches and the sample on the other hand. The [1 0 0] direction is perpendicular to the *z*-axis for the graphite foil between the sample and the punches whereas it is parallel to the *z*-axis for the graphite foil between the sample and the die. Its high thermal conductivity along [1 0 0] enhances the heat losses outside. On the contrary, because of its poor thermal conductivity along [0 0 1], the foil reduces the heat exchanges between the die and the sample and between the punches and the sample.

The energy balance on the whole system determines the electric power delivered by the SPS apparatus (P_{el}) to the system within the time Δt and can be expressed as follows:

$$P_{el}\Delta t = E_{J\,die\,(if\,graphite)} + E_{J\,punches} + E_{J\,sample} + E_{th\,punches\leftrightarrow sample} + E_{th\,punches\leftrightarrow die} + E_{th*\,punches\rightarrow outside} + E_{th\,die\leftrightarrow sample} + E_{th*\,die\rightarrow outside} \quad (1)$$

Electric power (P_{el}) is defined as the energy quantity delivered by time unit by the SPS apparatus to the system. E_J is the energy released by Joule effect from the electrically conducting elements of the system. E_{th} is the thermal energy transferred by conduction between the different system parts. E_{th^*} is the thermal energy transferred by radiation.

The carbon felt surrounding the mould reduces heat exchanges between the mould and outside. So, the term related to the radial heat transfer from the die to outside is not considered. Only the term related to the axial heat transfer from the die to outside is taken into account because the die upper and bottom are not recovered. In most setups (when graphite die is used), this term is constant because the die section does not change. On the other hand, the thermal energy transferred by radiation of the punches is only radial. This term is not constant from one setup to another because the punch temperature may change. However, according to the temperature and the punch dimensions concerned, which are at a low level for radiation losses, a difference of punch temperature does not involve a large discrepancy between the radiation losses.

The die and punch dimensions (with 20 mm height for the punches) are defined such as the punch resistance is higher than that of the die. Due to the fact that an equivalent or a higher current flows through them, the Joule effect is larger in the punches than in the die. Moreover, Matsugi et al. [8] have reported that independently of the powder, the maximum temperature of the system is always in the punches. However, Anselmi-Tamburini et al. [14] have shown that it is true initially only because after the system temperature distribution becomes homogeneous. Consequently, the heat transfer from the die to the punches can be neglected.

An axial thermal gradient is created due to the maximum system temperature located at the punches. Ozaki et al. [19] have observed that in an aluminium sample, the centre densification is lower than the surface densification. So, the heat transfer from the sample to the punches may be not taken into account.

During the sintering of a conducting material, the current flows through the punches, the die (if graphite) and the sample. Due to the fact that the current distribution is function of the electric resistance difference between the die and the sample, the current flows mainly through the nickel sample, and consequently, its Joule effect is greater than that of the die. This is confirmed by temperature measurements, performed by Tomino et al. [20] in the case of the sintering of a copper powder, which indicate a higher sample temperature than that of the die. So, the heat transfer from the die to the sample is not taken into account.

The Eq. (1) can be finally rewritten as:

$$\begin{aligned} P_{\mathrm{el}}\Delta t = {} & E_{\mathrm{J\,die\,(if\,graphite)}} + E_{\mathrm{J\,punches}} + E_{\mathrm{J\,sample}} \\ & + E_{\mathrm{th\,punches}\rightarrow\mathrm{sample}} + E_{\mathrm{th\,punches}\rightarrow\mathrm{die}} \\ & + E_{\mathrm{th*\,punches\,(radial)}\rightarrow\mathrm{outside}} + E_{\mathrm{th\,sample}\rightarrow\mathrm{die}} \\ & + E_{\mathrm{th*\,die\,(axial)}\rightarrow\mathrm{outside}} \end{aligned} \quad (2)$$

Eq. (2) supports the explanation that, for a set sintering temperature, an evolution of the electric power delivered may lead to an evolution of the heat received by the sample. So, the discrepancy of the heat really received by the sample with the expected one due to the sintering cycle could explain the microstructure variations. The discussion is voluntarily focused on the die heating and not on the sample heating because the response of the machine in terms of electric power depends on the temperature measured by a thermocouple set in the die and not in the sample.

4.2. Influence of the mould setup

The nickel sample is generally heated by Joule effect and heat transfer from punches, excepted in the setup 3 where the sample is only heated by heat transfer from the die. The die is heated by Joule effect and by heat transfer from punches and sample when graphite made (setup 1). It is only heated by this heat transfer (from punches and sample) when alumina made (setup 2) and, finally by Joule effect and heat transfer from punches when the sample is electrically and thermally insulated (setup 3).

Fig. 3 shows that the set temperature is more easily reached when the die is heated by Joule effect (setup 3) than by heat transfer from the sample (setup 2). Indeed, a lower electric power is required. The lower electric power means that, for a time interval, the thermal energy of the whole system is diminished. In addition, in this setup 3, the sample is not a heat source (no Joule effect) and is heated only by the die, leading to a real temperature of the nickel sample lower in spite of a same set temperature (inside the die). That may explain that the sintered sample in the setup 3 is the least dense of the three.

The setup 1 requires the highest electric power of the three setups. So, the Joule effect of the graphite die in the setup 1 although present, is too weak, compared with that of the setup 3, to heat as easily the similar die volume. Indeed, the current can also flow into the sample in the setup 1. Compared to the setup 2, although there is a Joule effect of the die in the setup 1, the set temperature is with more difficulty reached. Indeed, the whole die volume is heated when the sample is sintered in a graphite die (setup 1), whereas the die volume heated is limited to the area nearest to the sample in the setup 2, due to the poor thermal conductivity of the alumina die. The thermal energy of the whole system in the setup 1 is therefore increased. However, as the electric power delivered in the setup 1 is not only used, as in the setup 2, to heat the sample by Joule effect, a lower density is obtained. As the electric power delivered in the setup 1 is partly used to heat the sample by Joule effect, compared to the setup 3, a higher density is obtained.

In the setup 2, the electric power peak (Fig. 3) due to the cracking of the alumina die, is responsible of an additional Joule heat in the system, which may contribute to increase the sample density. However, the shrinkage of the sample sintered in an alumina die (Fig. 4) starts at lower temperature compared to a specimen sintered in a graphite mould. Consequently, the sample in the setup 2 is heated more efficiently since the beginning of the cycle and probably would have exhibited the highest density without the additional Joule heat due to the electric power peak.

4.3. Influence of the graphite foil setup

When the nickel is sintered under 70 MPa, the Joule effect of the die being negligible, the die is mainly heated by heat transfer from the sample and the punches [17].

In the setup 4, the graphite foil enhances the heat transfer from the punches to the die (non-existent in the setup 5 because no physical contact between punches and die exists). A lower electric power is consequently expected. However, the graphite foil reduces the heat transfer from the sample towards the die because its insertion creates a thermal barrier. That is why the electric power delivered in the setup 4 is not lower than that delivered in the setup 5. In addition, the heat transfers from the punches to the die in the setup 4 reduce those from the punches to the sample. Such a feature combined with an equivalent electric power delivered leads to a microstructure slightly finer of the sample sintered in the setup 4.

In the setup 5, due to an increase of the system resistance by the insertion of graphite foils between the punches and the sample, it is necessary to deliver an electric power lower than in the setup 6. This smaller electric power reduces the Joule effects of the punches and of the sample. Moreover, the thermal energy produced by the punches is partially transmitted to the sample when the graphite foil is inserted between the punches and the sample. That is why the sample microstructure is finer in the setup 5.

When the nickel is sintered under 30 MPa, the sample is more resistive [21,22]. Consequently the Joule effect of the die is not anymore negligible. So the graphite foil enhances the current flow in the die, what increases its Joule effect in setups 4 and 5. However, because of its high thermal conductivity along [1 0 0], the graphite foil between the die and the sample leads in the setup 4 to thermal dissipations, which are non-existent in the setup 5. That is why the electric power delivered in the setup 4 is higher than in the setup 5. Moreover, we may consider that the current repartition between the die and the sample is identical in setups 4 and 5. Indeed, the variation of electric power results probably from the heat dissipated by the graphite foil inserted between the die and the sample (setup 4). Consequently, the Joule effect of the samples is considered identical in the setups 4 and 5, what leads to close microstructures. The electric power required for the setup 6 is larger than for the setup 5 because there is for the latter a Joule effect of the die that there is not for the first one. As the current flows totally through the sample when no graphite foil is used (setup 6), a coarser microstructure of samples sintered in such a setup is expected. However because of small variations of electric power (29% maximum), the grain size is only slightly different.

5. Conclusion

Although the set temperature is identical for all the investigated setups, the densification of a nickel specimen heated by Joule

effect (in an alumina die) is larger than that of a nickel specimen heated by thermal conduction (in the graphite die with alumina spacers). The repartition of the graphite foil does not influence the microstructure of nickel specimens because the sample heating is mainly ensured by Joule effect. Indeed, this observation is not anymore proper for ceramic material like alumina. In this case, a finer microstructure is obtained when the sample is separated from the die by a graphite foil [23].

Acknowledgements

The authors would like to thank the DGA for funding this research through a PhD grant. We would also like to acknowledge the advice provided by Dr. G. Nicolas (Plansee) and H. Couque (Nexter Munitions).

References

[1] M. Tokita, International Symposium on Functionally Graded Materials, Tokyo, 1999.
[2] Z.A. Munir, M. Ohyanagi, M. Tokita, M. Khor, T. Hirai, U. Anselmi-Tamburini, Ceramics Transactions 194, Proceedings of the 6th Pacific Rim Conference on Ceramics and Glass Technology, Hawaii, 2006.
[3] R. Orru, R. Licheri, A.M. Locci, A. Cincotti, G. Cao, Mater. Sci. Eng. R 63 (2009) 127–287.
[4] J.R. Groza, A. Zavaliangos, Mater. Sci. Eng. A 287 (2000) 171–177.
[5] T. Grosdidier, G. Ji, F. Bernard, E. Gaffet, Z.A. Munir, S. Launois, Intermetallics 14 (2006) 1208–1213.
[6] N. Millot, S. Le Gallet, D. Aymes, Y. Grin, F. Bernard, J. Eur. Ceram. Soc. 27 (2007) 921–926.
[7] Z.H. Zhang, F.C. Wang, L. Wang, S.K. Li, M.W. Shen, S. Osamu, Mater. Character. 59 (2008) 329–333.
[8] K. Matsugi, H. Kuramoto, T. Hatayama, O. Yanagisawa, J. Mater. Process Technol. 146 (2004) 274–281.
[9] A. Kamiya, J. Mater. Sci. Lett. 17 (1998) 49–51.
[10] J. Schmidt, PhD thesis, Technischen Universität Dresden, 2003.
[11] Z. Shen, H. Peng, J. Liu, M. Nygren, J. Eur. Ceram. Soc. 24 (2004) 3447–3452.
[12] J. Rathel, M. Herrmann, W. Beckert, J. Eur. Ceram. Soc. 29 (2009) 1419–1425.
[13] K. Vanmeensel, A. Laptev, J. Hennicke, J. Vleugels, O. Van der Biest, Acta Mater. 53 (2005) 4379–4388.
[14] U. Anselmi-Tamburini, S. Gennari, J.E. Garay, Z.A. Munir, Mater. Sci. Eng. A 394 (2005) 139–148.
[15] K. Vanmeensel, A. Laptev, O. Van der Biest, J. Vleugels, J. Eur. Ceram. Soc. 27 (2007) 979–985.
[16] A. Zavaliangos, J. Zhang, M. Krammer, J.R. Groza, Mater. Sci. Eng. A 379 (2004) 218–228.
[17] S.W. Wang, L.D. Chen, Y.S. Kang, N. Niino, T. Hirai, Mater. Res. Bull. 35 (2000) 619–628.
[18] V.Y. Kodash, J.R. Groza, K.C. Cho, B.R. Klotz, R.J. Dowding, Mater. Sci. Eng. A 385 (2004) 367–371.
[19] K. Ozaki, K. Kobayashi, T. Nishio, A. Matsumoto, A. Sugiyama, J. Jpn. Soc. Powder Powder Metall. 47 (2000) 293–297.
[20] H. Tomino, H. Watanabe, Y. Kondo, J. Jpn. Soc. Powder Powder Metall. 44 (1997) 974–979.
[21] C. Argento, D. Bouvard, Int. J. Heat Mass Transfer 39 (1996) 1343–1350.
[22] J.R. Groza, A. Zavaliangos, Rev. Adv. Mater. Sci. 5 (2003) 24–33.
[23] L. Minier, PhD thesis, University of Burgundy, France, 2008.